Phytomedicine 103 (2022) 154228

Contents lists available at ScienceDirect

Phytomedicine

journal homepage: www.elsevier.com/locate/phymed

Original Article

Viola yedoensis Makino formula alleviates DNCB-induced atopic dermatitis by activating JAK2/STAT3 signaling pathway and promoting M2 macrophages polarization

Hairong Zeng [a,b,1], Bei Zhao [b,1], Die Zhang [a,1], Xin Rui [c,1], Xudong Hou [b], Xingxing Chen [a], Benrui Zhang [d], Yi Yuan [a,*], Hongping Deng [b,*], Guangbo Ge [b,*]

[a] *Putuo Hospital, Shanghai University of Traditional Chinese Medicine, Shanghai 200062, China*
[b] *Shanghai Frontiers Science Center of TCM Chemical Biology, Institute of Interdisciplinary Integrative Medicine Research, Shanghai University of Traditional Chinese Medicine, Shanghai, 201203, China*
[c] *Baoshan Branch, Shuguang Hospital Affiliated to Shanghai University of Traditional Chinese Medicine, Shanghai, China*
[d] *Shanghai University of Traditional Chinese Medicine, Shanghai 200062, China*

ARTICLE INFO

Keywords:
Viola yedoensis Makino (VYAC)
Atopic dermatitis
Anti-inflammatory
Macrophages polarization
JAK2/STAT3 signaling pathway
Traditional Chinese medicine

ABSTRACT

Background: Atopic dermatitis (AD), a common inflammatory skin disorder, severely affects the life quality of patients and renders heavy financial burden on patient's family. The Chinese medicine *Viola yedoensis* Makino formula (VYAC) has been widely used for treating various skin disorders. Previous studies have reported that VYAC is effective in relieving DNCB-induced AD and inflammation. However, the anti-inflammatory mechanism of VYAC is still ill-defined and poorly understood. This study aims to investigate the therapeutic effects of VYAC on DNCB-induced AD and to elucidate the underlying anti-inflammatory mechanisms.

Methodology: VYAC were extracted with 70% ethanol and lyophilized for use. AD mice were established by DNCB. The therapeutic effects of VYAC were evaluated by oral administration VYAC (150, 300 and 600 mg/kg) daily *in vivo*. The histopathological and immunohistochemistry were used to analyze skin lesion and macrophages infiltration, RT-qPCR and Elisa were used to analyze the inflammatory factors in skin tissues and serum. To explore the underlying mechanism of VYAC against AD *in vitro*. RAW264.7 cells and bone-marrow-derived macrophages (BMDMs) were employed for macrophage polarization analysis. Flow cytometer, immunofluorescence and western blot were used to analyze M2 macrophages markers. STAT3 siRNA were transfected into both cells to validate the effects of VYAC-induced macrophages M2 polarization via JAK2/STAT3 signaling pathway.

Results: VYAC ameliorated skin lesion of DNCB-induced AD mice by decreased clinical scores and epidermal thickness, decreased the level of pro-inflammatory factors (IL-1β, TNF-α and IL-18) and enhanced IL-10 anti-inflammatory factor level, inhibited macrophages infiltration and promoted M2 macrophages polarization *in vivo*. VYAC significantly promoted M2 macrophages polarization *in vitro*. It is observed that VYAC not only inhibited the phosphorylation of JAK2 and STAT3 in RAW264.7 cells and BMDMs, but also accelerated the translocation to the nucleus. What's more, VYAC reduced the polarization of M2 macrophage by activating JAK2/STAT3 signaling pathway was observed in both cells.

Conclusions: Our findings demonstrate that VYAC significantly ameliorates skin lesion of DNCB-induced AD mice and reduces the levels of inflammatory factors by activating JAK2/STAT3 signaling pathway and promoting M2 macrophages polarization.

Abbreviations: AD, Atopic dermatitis; BMDM, bone-marrow-derived macrophages; DMEM, DuIbecco's modified eagIe's medium; DNCB, dinitrochlorobenzene; DXM, dexamethasone; ECL, enhanced chemiluminescence reagents; FCM, flow cytometry; FBS, fatal bovine serun; IHC, immunohistochemistry; IF, immunofluorescence; IFN-γ, interferon-γ; IL-1β, interleukin-1β; IL-18, interleukin-18; IL-10, interleukin-10; JAK2, Janus Kinase 2; LPS, lipopolysaccharide; LC-MS, liquid chromatography-tandem mass spectrometry; M1, classically activated macrophages; M2, alternatively activated macrophages; M-CSF, macrophage colony-stimulating factorMakino.

* Corresponding authors.
E-mail addresses: yuanyi0625@163.com (Y. Yuan), hpdeng@shutcm.edu.cn (H. Deng), geguangbo@shutcm.edu.cn (G. Ge).
[1] These authors have contributed equally to this work and share first authorship

https://doi.org/10.1016/j.phymed.2022.154228
Received 18 February 2022; Received in revised form 20 May 2022; Accepted 31 May 2022
Available online 2 June 2022
0944-7113/© 2022 Elsevier GmbH. All rights reserved.

Introduction

Atopic dermatitis (AD), a typical inflammatory skin disorders, displays sensitive and dry skin, localized or disseminated lesions, and accompanied by chronical recurrent and severe itching symptoms (Bieber T., 2021). The prevalence of AD is increasing and has been considered a public health problem (Wallach and Taïeb., 2014). Approximately 10% of children and 2–5% adults were diagnosed with AD (Girolomoni et al., 2021). AD is a chronic recurrent inflammatory disease, whose pathogenesis is still not completely clear. It is usually thought to be concerned with environmental factors, genetic predisposition, skin barrier dysfunction and immunological abnormalities (Gür Çetinkaya and Şahiner., 2019; Campana et al., 2017). Family history is the strongest risk factor for AD developing, about 75% in twin appears (Thomsen et al., 2007). What's more, the mutation of filaggrin (FLG), a gene encodes the preprotein pro-filaggrin considers as a primary driver of AD (McAleer and Irvine., 2013). It is 3–5 times higher risk of AD in individuals than thus who do not have FLG function mutations (Irvine et al., 2011). Disruption of skin barrier function in AD increased permeability, elevated epidermal water loss and pH, and altered lipid composition, further damaged skin microbial, activated keratinocytes to release proinflammatory and pruritogenic signals, resulting in tissues damage and type 2 inflammatory cells recruiting (Tsakok et al., 2019; Halling-Overgaard et al., 2017). Immunological abnormalities are pivotal to the pathogenesis of AD, with T-cells, dendritic cells, and macrophages infiltrate to release pro-inflammatory factors (TNF-α, IL-1β) and to downregulate Th2-associated (IL-4 and IL-10) expression has been deemed to involve in the immune dysregulation in AD (Weidinger et al., 2018).

To dermatologists, general practitioners and pediatricians, AD is easily diagnosed by clinical examination on the basis of morphological features of lesions. Unfortunately, no laboratory and pathological markers specific of AD restricted clinical treatment (Bos et al., 1998; Saeki et al., 2009). Current treatment of AD is to alleviate symptoms by avoidance trigger factors and by establish long-term disease control, and urgent affairs are skin barrier restoration and reducing inflammation. Moisturizers, which can increase hydration and reduce xerosis, itch is useful for improve barrier function (Hon et al., 2018). Topical corticosteroids for anti-inflammatory and topical calcineurin inhibitors (tacrolimus and pimecrolimus) for reduced clinical efficacy are diffusely deemed to as the first-line treatment drugs (Weidinger et al., 2017). Besides, crisaborole ointment, an inhibitor of the intracellular enzyme phosphodiesterase 4, was approved by FDA in 2016 for aged 2 years or older AD patients (Ahmed et al., 2018). In addition, delgocitinib 0.5% ointment has recently been approved for adults AD patients in Japan (Nakagawa et al., 2020). In spite of easy diagnosis and effective treatment, AD severely affects patient's life quality and renders patient's family heavy financial burden.

Macrophage, which acts as antigen-presenting cells, plays a vital role in the pathogenesis of AD (Zeng et al., 2020; Nakai., 2021). Macrophages, part of the immune system regulating inflammatory response and tissue remodeling, were accumulated in acutely and chronically in inflamed lesions (Qader et al., 2021). Macrophages display different polarization phenotype (M1 or M2 macrophages) in answering to microenvironments of lesion skin (Zeng et al., 2020). M1 macrophages usually called pro-inflammatory subtype, were induced by lipopolysaccharide (LPS) and interferon-γ (IFN-γ) and produced pro-inflammatory cytokines (such as TNF-α, IF-1β, IL-10). In contrast, M2 macrophages usually called anti-inflammatory subtype, were induced IL-4 or IL-13 and produced anti-inflammatory cytokines (such as IL-10) (Hristodorov et al., 2015). Successful switch from M1 to M2 was considered to be an effective way to treat AD.

Macrophage's polarization was regulated by various molecular mechanism. Previous research proved that JAK2/STAT3 signaling pathway is vital in macrophages polarization and activation (de Jonge et al., 2005). Practically, STAT3 would dimerize after activated by phosphorylation of serine (Ser) 727 and tyrosine (Tyr) 705 and translocated into nucleus, thereby boding to promoter region of target genes and activating their transcription, resulting in M2 macrophages polarization (Yu et al., 2016; Zhang et., 2017). Kong et al. (Kong et al., 2019), have confirmed that Hesperetin derivative-12 (HDND-12) promotes M2 macrophage polarization via JAK2/STAT3 signaling pathway. Yuan, et al. (Yuan et al., 2014), have proved that cigarette smoke extract mediated M2 macrophage polarization through JAK2/STAT3 signaling pathway. Macrophage polarization played a vital in the development of AD, thus searching the drugs which could switch macrophage from M1 to M2 polarization has great significance.

Viola yedoensis Makino formula (VYAC), a clinical prescription for skin disease, had successfully treated hundreds of thousands of patients. It consists of three herbs including *Viola yedoensis* Makino (Violaceae, Viola, herb), *Sophora flavescens* Aiton (Fabaceae, Sophora, root) and *Dictamnus dasycarpus* Turcz (Rutaceae, Dictamnus, root and rhizome). Previous studies found that VYAC could inhibit inflammatory cytokines production *in vitro*, and ameliorate DNCB-induced AD *in vivo* (Zeng et al., 2016, 2021). However, the underlying anti-inflammatory mechanisms of VYAC for AD are still not clear. Thus, the aims of this study were to investigate the therapeutic effects of VYAC on DNCB-induced AD and to elucidate the underlying anti-inflammatory mechanisms of this Chinese medicine.

Materials and methods

Chemicals and reagents

DNCB and DXM were purchased form sigma (MO, usa), BCA protein assay kit was purchased from Thermo Fisher Scientific (Waltham, MA, USA), The primary antibodies against JAK2 (#3230), p-JAK2 (Tyr1008) (#8082), STAT3(#4904), p-STAT3(Tyr705) (#9145), GAPDH (#5174) and the second antibody (#7074) were purchased from CST (MA, USA), Lamin A and Tubulin were bought from Santa Cruz Biotechnology (Shanghai) Co., Ltd. (Shanghai, China). Fluorochrome-conjugated antibody CD11b-percp-Cy5.5, CD11c-FITC and Ly6G-PE, CD206-PC7 and CD86-FITC were purchased from Thermo Fisher Scientific (Waltham, MA, USA). TNF-α, IL-1β, IL-18 and IL-10 ELIA kit were obtained from Abcam (Shanghai, China).

Plant extraction preparation and chemical profile of vyac formula

The crude decoction consists of three herbs (*Viola yedoensis* Makino, *Sophora flavescens* Aiton and *Dictamnus dasycarpus* Turcz) according to the weight ratio of 2:1:1, were authenticated by Prof. Jun-song Li (Shanghai University of TCM). The *Viola yedoensis* Makino formula extract was prepared according to previously method (Zeng et al., 2021). Briefly, the herbs were extracted and refluxed with 70% ethanol, and then the extract was filtered and concentrated to dried powder and stored in −20 °C for further use.

LC-MS for VYAC formula was conducted as earlier described (Zeng et al., 2021). Generally, we used LC 20ADXR system, AB-SCIEX 5600 Triple TOF MS and C18 column (2.0 × 250 mm, 5 μm) with 10 μl injection volume and 0.5 ml/min flow rate of mobile phase (0.1% formic acid and acetonitrile) for chromatographic segregation. The optimized parameters of mass spectrometry were as previous study (Zhang et al., 2021). The searching ranges of the precursor ion was 100–2000 *m/z* and the components were identified with error ppm (±5).

Animal tests

Female BABL/c mice (6–8 weeks old, and 20 ± 2 g weight) were obtained from Shanghai University of Traditional Chinese Medicine. All mice were kept on standard environment (temperature 22±1 °C, humidity 40–60%), free to water/food and 12 h of light/dark cycle. The animal procedures were approved by Committee of Shanghai University

of Traditional Chinese Medicine (certification number: SYXK, 2014–0008)

AD models and drug treatment

AD mice were established according to previous study (Zeng et al., 2021). Briefly, 2 cm x 2 cm area of dorsal was shaved by electric shaver. Then 100 μl 0.5% DNCB was applied on the first three days to sensitized, further, 100 μl 0.3% DNCB was applied every other two days. The control group mice were applied with equal vehicle (acetone/olive 3:1, vol/vol).

Six groups ($n = 8$) consist of control group, AD model group, VYAC treated group (150, 300, 600 mg/kg) and DXM group (mg/kg). For VYAC treated group, the mice were intragastric (ig) administration every day. For DXM group (positive control), the mice were intraperitoneally injected with 2.5 mg/kg DXM every three days. Control group and AD model group were given the same amount of vehicle. The skin lesion features (erythema, edema, crusts and excoriations) were observed every day. The scoring criteria of the mice AD model were based on the clinical symptom severity to conduct an objective scoring system. The clinical score was recorded (0 no symptoms, 1 mile, 2 intermediate and 3 severe). At the end of experiment, the blood was collected and dorsal skin was isolated.

Histopathological analysis

For histological analysis, fixed skin tissues were embedded with paraffin and sectioned at suitable thickness, followed by Hematoxylin- and eosin stain according to protocols. The epidermal thickness was obtained from pathologist.

ELISA

Serum cytokines (IL-1β, TNF-α, IL-18 and IL-10) were detected by ELISA kit. Shortly, serum was collected, and the cytokines were detected according to the manufacturer's instruction.

Cell culture

RAW264.7 (monocyte-derived macrophage cell line) was got from Cell Bank of Chinese Academy of Science, and cultured in DMEM (meilune) containing 10% (vol/vol) FBS (Gbico) at a humidified incubator. Bone-marrow-derived macrophages (BMDMs) cultured in DMEM (meilune) containing 10% (vol/vol) FBS (Gbico) and M-CSF (50 ng/ml) at a humidified incubator for 7 days to get mature BMDMs.

Bone-marrow-derived macrophages (BMDMs) isolation

BMDMs separation as previously described (Trouplin et al., 2013). Concisely, BABL/c mice legs were newly collected, removed skin and muscles and soaked in 75% ethanol for minutes immediately, washed with refrigerated PBS 3 times. After that, the bone marrow was blown out of the femur using a 1 ml syringe, and filtered with a nylon mesh cell strainer. Further blood cell lysis buffer was added and centrifuged at 450 g for 10 mins. Then the cells were cultured with macrophage colony-stimulating factor (M-CSF) to obtain mature BMDMs.

Macrophage polarization analysis

RAW264.7 and mature BMDMs cells were seeded in 6-well plates, and treatment with drug of different concentrations, IL-13 (10 ng/ml, PEPROTECH) was selected as positive control for M2 macrophages polarization. Then the cells were through polarization analysis using qRT-PCR, western blot and flow cytometry.

Cells transfection with STAT3 siRNA plasmid

RAW264.7 cells were seeded in 6-well plates with a density of 5×10^5 cell per well, then STAT3 plasmid (GenePharma, Shanghai) were transfected into cells with Lipofectamine 3000. The sequences of plasmid were shown **in table S2**. After 24 h transfection, the cells were used for further study.

RNA isolation and RT-qPCR

Total RNA from skin tissues and cells were extracted using Trizol reagent (Invitrogen), and cDNA was synthesized using real-time reagent kit (Takara, Japan), qPCR analysis was performed by SYBR Premix Ex TaqTM II (Takara, Japan) in a Vii A 7 Dx system (Applied Biosystems, USA). The data was normalized to GAPDH and analyzed using $2^{-\triangle\triangle Ct}$ approach. The primers were seen in table S3.

Flow cytometry (FCM)

The lymph nodes of mice were isolated and single cell suspension was prepared by red blood lysis. The single cell was stained with fluorochrome-conjugated antibody (CD11b-percp-Cy5.5, CD11c-FITC and Ly6G-PE). Fluorochrome-conjugated antibody (CD206-PC7 and CD86-FITC) were also used to stain RAW264.7 cells. Then the stained cells were analyzed by flow cytometer and data analyzed via FlowJo 10.0 software.

Immunoblotting

Protein was collected, then quantitated by BCA kit, further separated by SDS-PAGE and transferred to PVDF membrane, in the following step blocked by 5% non-fat milk and incubated with primary antibody STAT3 (1:1000), p-STAT3 (1:1000), JAK2(1:1000), p-JAK2(1:1000) and GAPDH (1:2000) overnight at 4 °C. After that, the membrane was incubated with HRP-linker second antibody (1:5000) at room temperature. Finally, Enhanced chemiluminescence reagents (ECL) was used for bands detection, and image J software was used for protein quantified.

Immunohistochemistry (IHC) and immunofluorescence (IF)

Skin tissues Immunohistochemistry analysis was performed as previously described (Zeng et al., 2021). Briefly, tissues were fixed and embedded in paraffin, then dewaxed with xylene, dehydrated with ethanol, antigen retrieval with citrate buffer and blocked with 10% goat serum. In the next step, it was incubated with primary antibody of F4/80 and CD206 overnight at 4 °C. followed by secondary antibody at room temperature. Cells immunofluorescence analysis was performed as previous way (Zhang et al., 2017). Briefly, RAW264.7 cells were fixed after treatment, then used 0.2% triton X-100 for permeabilized, further, blocked with 5%BSA. After that, it was incubated with primary antibody of p-STAT3 overnight at 4 °C, followed by incubated with fluorochrome-conjugated secondary antibody and stained with DAPI for nuclei. Finally, imaged under a confocal microscope.

Statistical analyses

Data are expressed as mean± standard (mean ± SD), and analyzed by one-way analysis of variance (ANOVA), followed by an appropriate *post hoc* test. The difference between two groups was performed using unpaired student's *t-test*. GraphPad Prism software was used to perform the statistical analysis (Version 4.0 GraphPad Software, Inc., San Diego, CA) $p \leq 0.05$ was considered statistically significant.

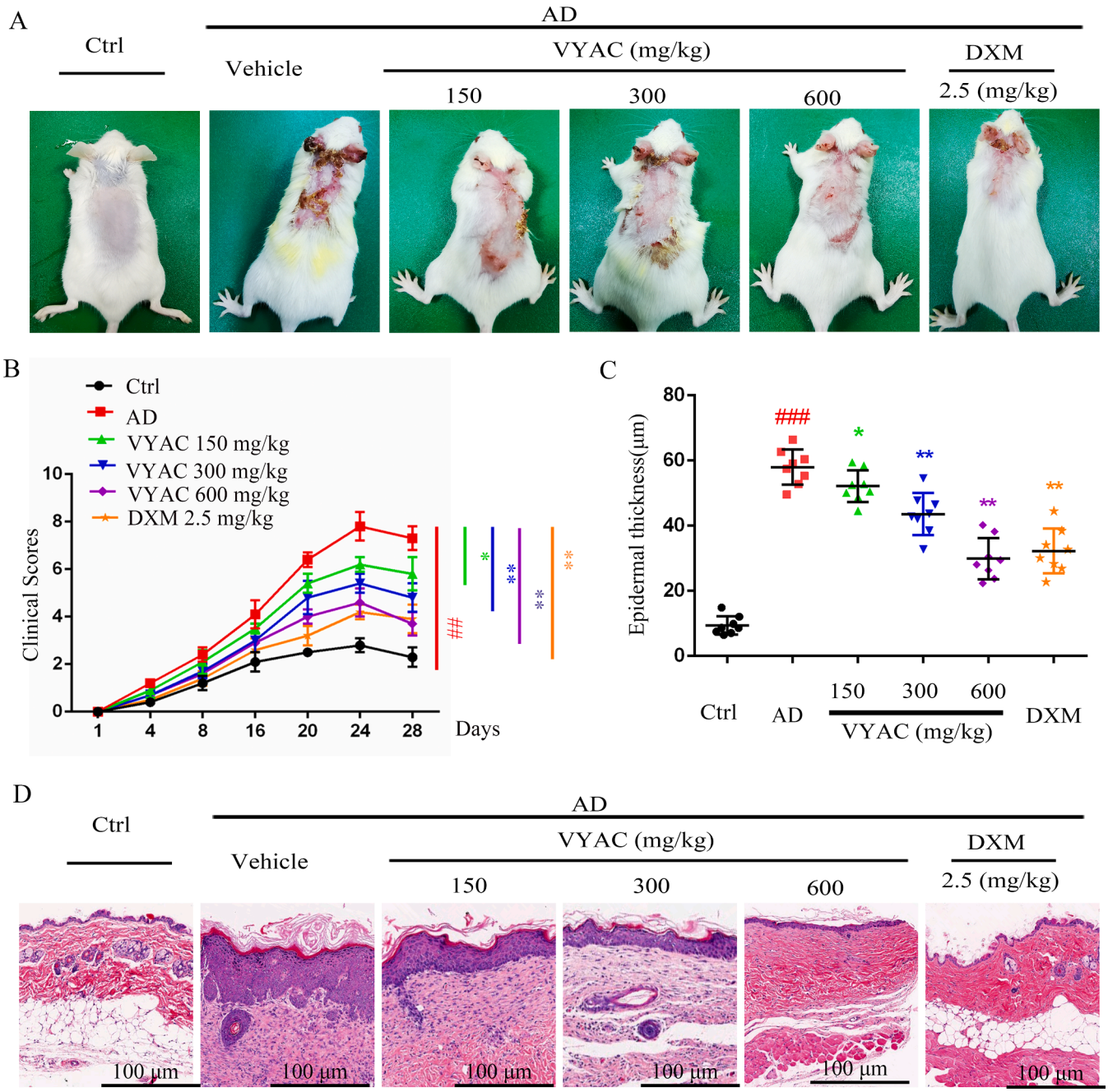

Fig. 1. VYAC ameliorated DNCB-induce AD mice skin lesion. (A) Photographs for the dorsal skin lesion of mice in different groups. (B) Clinical scores of skin lesion in different groups. (C) Epidermis thickness of skin lesion in different groups. (D) Histopathological features of skin lesion in different groups, the skin was stained by H&E (magnification 200X, scale bar 100 μm). Data are shown as mean ± SD ($n = 8$). $^{\#\#}p < 0.01$ and $^{\#\#\#}p < 0.001$ *vs.* Control group (Ctrl); $^{*}p < 0.05$ and $^{**}p < 0.01$ *vs.* AD model group (Vehicle).

Results

Chemical profiling for VYAC

According to literature and Chinese herb database, LC-MS/MS was employed for matching components in the database (Fig. S1). By using LC-MS/MS technique, we discovered 119 components in VYAC through retention time comparative analyses in comparison with the reference standards (Table S1). Detailed analysis and category revealed that the identified major constituents in VYAC were consistent with the results from a previous literature (Zeng et al., 2021).

VYAC ameliorates skin lesion of DNCB-induce AD mice

To investigate the impact of VYAC on DNCB-induced AD mice dorsal skin lesion, the typical features, such as erythema, edema and excoriations, of AD were monitored every day (Fig. 1). In AD model group, the mice skin lesion was more obvious with erythema, crusts, edema and excoriations during the experiment period, compared to control group mice. However, VYAC treatment groups (150, 300, 600 mg/kg) showed effectively and significantly reduced symptoms, such as decreased erythema and scaling. What's more, high drug dosing (600 mg/kg) resulted in therapeutic efficiency similar to positive control of DXM (2.5 mg/kg) (Fig. 1A). Clinical scores also showed that, AD model group displayed higher clinical scores, conversely, VYAC treatment group (150, 300,

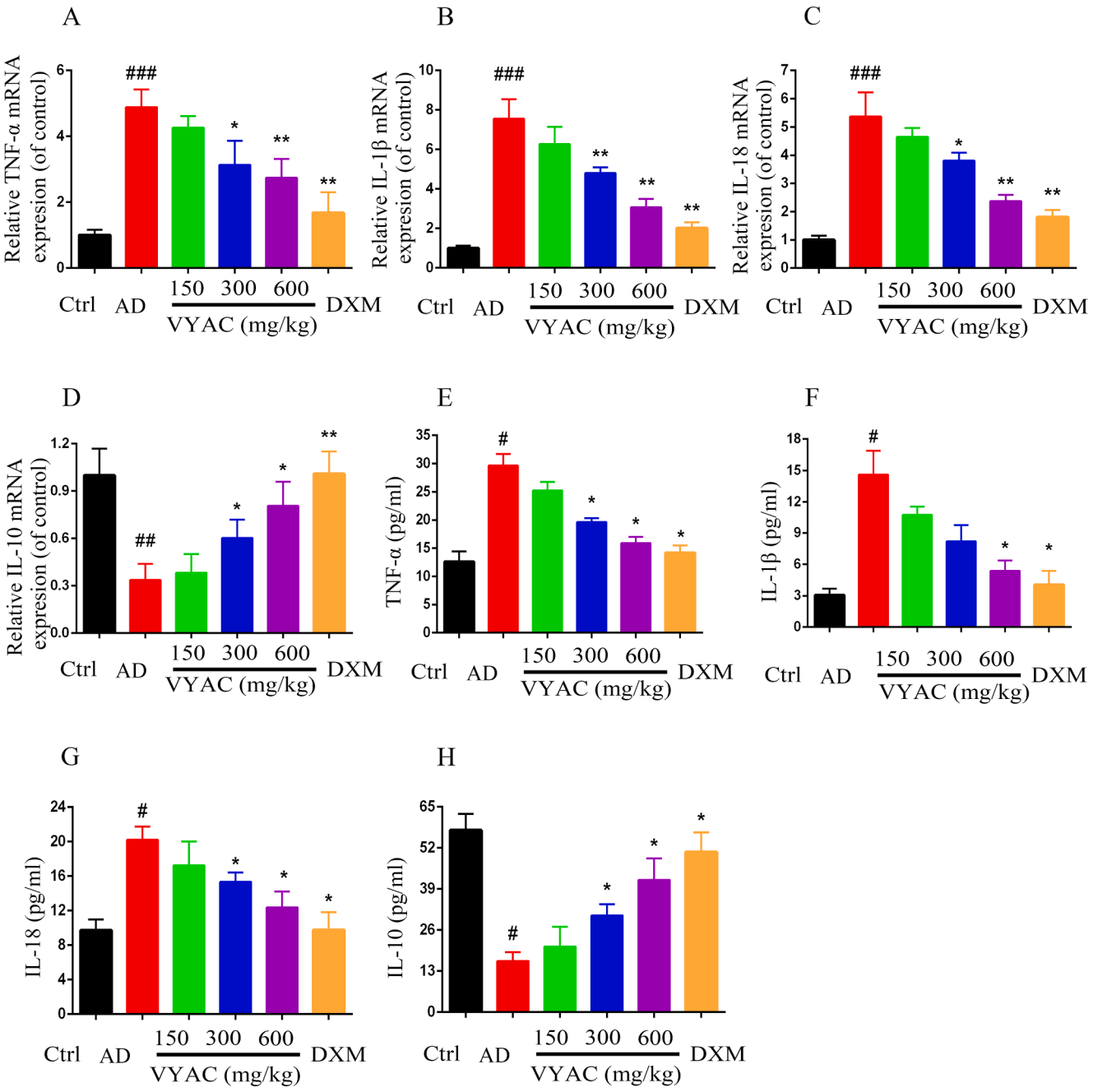

Fig. 2. VYAC decreased the level of proinflammatory factors in DNCB-induced AD mice. The mRNA levels of TNF-α (A), IL-1β (B) IL-18 (C) and IL-10 (D) in skin lesion were analyzed by qRT-PCR. The protein levels of TNF-α (E), IL-1β (F) IL-18 (G) and IL-10 (H) in serum were analyzed by ELISA kit. Data are shown as mean ± SD ($n = 3$). $^{\#}p < 0.05$, $^{\#\#}p < 0.01$ and $^{\#\#\#}p < 0.001$ *vs.* Control group (Ctrl); $^{*}p < 0.05$ and $^{**}p < 0.01$ *vs.* AD model group (Vehicle).

600 mg/kg) and DXM group (2.5 mg/kg) exhibited lower scores ($p < 0.05$) (Fig. 1B). Epidermal thickness was also a marker of skin lesion, the results showed that DNCB-induced AD mice showed a thicker epidermal, whereas, VYAC treatment group (150, 300, 600 mg/kg) and DXM group (2.5 mg/kg) significantly decreased epidermal thickness ($p < 0.05$) (Fig. 1C). Histopathological changes were further applied to indicate skin lesions, and epidermal/dermal hyperplasia with infiltrating inflammatory cells were observed in AD group. In contrast, VYAC treatment group (150, 300, 600 mg/kg) and DXM group (2.5 mg/kg) decreased the thickness of epidermal and inflammatory cell infiltration (Fig. 1D).

VYAC alleviates inflammation in AD mice

First, we detected the mRNA level of inflammatory factors in skin tissues. In AD mice, the mRNA levels of IL-1β, TNF-α and IL-18 were significantly increased compared with control group. While, the mRNA levels of IL-1β, TNF-α and IL-18 were significantly restrained after VYAC treatment via a dose-dependent manner ($p < 0.05$) (Fig. 2A, B and C). In contrast, IL-10, a M2 macrophages secreted anti-inflammation cytokine, the mRNA level was decreased in AD mice, and increased after VYAC treatment in a dose-dependent manner ($p < 0.05$) (Fig. 2D). Besides, the protein levels of TNF-α, IL-1β, IL-18 and IL-10 were explored in serum by ELISA. With VYAC dosing, the protein levels of IL-1β, TNF-α and IL-18 were decreased with similar trend as that of mRNA results (Fig. 2E and F). Meanwhile, the protein level of IL-10 was increased after VYAC treatment ($p < 0.05$) (Fig. 2G).

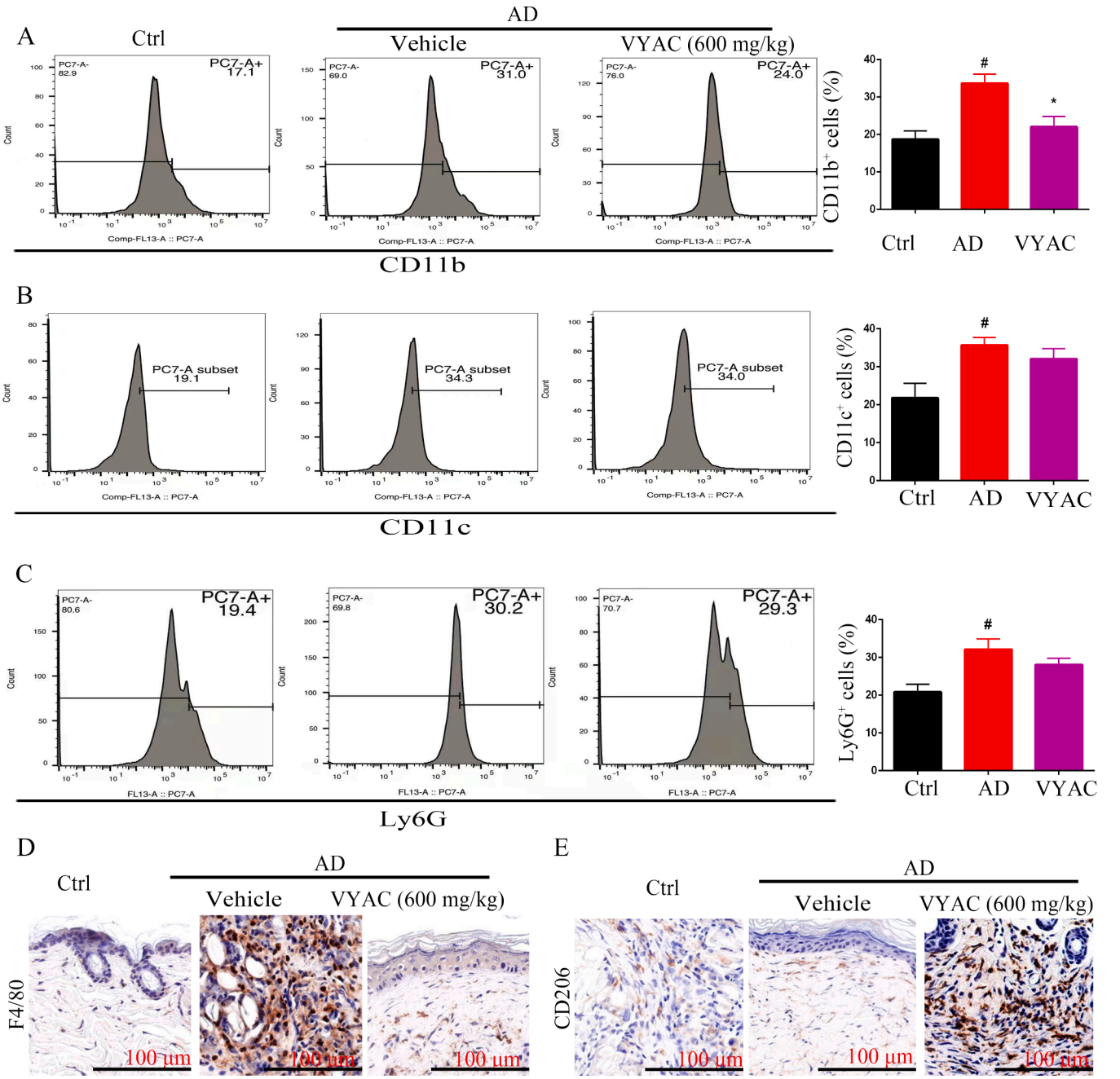

Fig. 3. VYAC inhibited infiltration macrophages in DNCB-induced AD mice. Single cell from lymph nodes was stained with fluorochrome-conjugated antibody CD11b-percp-Cy5.5 for macrophages (A), CD11c-FITC for dendritic cells (B) and Ly6G-PE for neutrophils (C). Macrophage infiltration and M2 Macrophage polarization in skin lesion were analyzed F4/80 (D) and CD206 (E) expression by immunohistochemistry. Data are shown as mean ± SD ($n = 3$). $^{\#\#}p < 0.01$ *vs.* Control group (Ctrl); $^{*}p < 0.05$ *vs.* AD model group (Vehicle).

VYAC inhibits infiltration macrophages in AD mice

Macrophage recruitment and infiltration is a key event in the development of AD (Lee et al., 2020). And AD model mice showed a large number of inflammatory cell infiltration and inflammatory factors secretion in results Fig 1D and Fig 2. So, we detected the immune-relate cells in axillary lymph nodes used flow cytometry. The results displayed that, compared with control group, AD mice $CD11b^+$ macrophages, $CD11C^+$ dendritic cells and $Ly6G^+$ neutrophils numbers were much higher ($p < 0.05$). However, VYAC 600 mg/kg only reduced the $CD11B^+$ macrophages numbers, little effects on $CD11C^+$ dendritic cells and $Ly6G^+$ neutrophils changes (Fig. 3A, B and C). Macrophage infiltration was also measured in skin tissues via immunochemistry. The results illustrated that the numbers of $F4/80^+$ macrophages (total macrophages) in AD mice were higher than the normal control group, the numbers of $F4/80^+$ macrophages (total macrophages) in VYAC (600 mg/kg) treated group were lower than AD group (Fig. 3D). However, the numbers of $CD206^+$ macrophages (M2 macrophages) were significantly increased in VYAC 600 mg/kg treated group (Fig. 3E).

VYAC prompts M2 macrophages polarization in RAW264.7 cells

It is well-known that M1 and M2 macrophages polarization is very important in the progression of AD (Zeng et al., 2020; Karuppagounder et al., 2016). Thus, we investigated whether VYAC could modulate macrophages polarization in RAW264.7 cells. First, we evaluated the

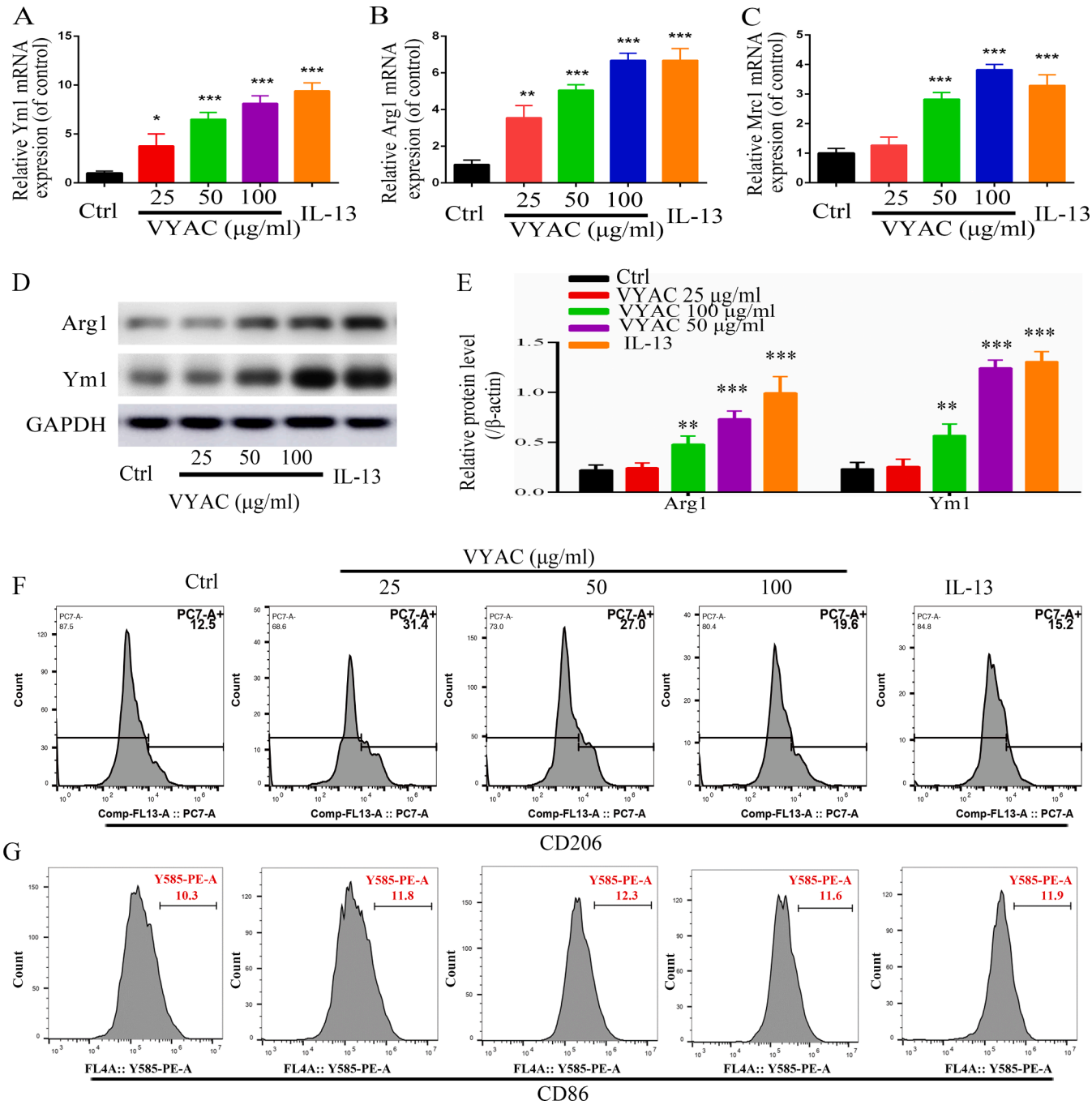

Fig. 4. VYAC promoted M2 macrophages polarization in RAW264.7 cells. RAW264.7 cells were treated with VYAC (25, 50 100 μg/ml) or IL-13 (10 ng/ml). qRT-PCR was used to analyze the mRNA level of M2 macrophages related genes Ym1 (A), Arg1 (B), Mrc1(C). Western blot was used to analyze the protein expression of M2 macrophages related protein Ym1 and Arg1 (D and E). Flow cytometry was used to analyze the percentage of M2 macrophages ($CD206^{+}$) and M1 macrophages ($CD86^{+}$). Data are shown as mean ± SD ($n = 3$). *$p <$ 0.05, **$p <$ 0.01 and ***$p <$ 0.001 *vs.* control group (Ctrl).

cytotoxicity of VYAC on RAW264.7 cells to determine the concentration. The viability of VYAC on RAW264.7 cells was not inhibited even at the dose of 800 μg/ml (Fig. S2 A). What's more, the viability has a little increase at the dose of 25, 50 and 100 μg/ml. So, we selected these dose *in vitro* experiments. Then, we used qRT-PCR to analyze the mRNA level of M2 macrophages related genes (Arg1, Ym1 and Mcr1). What's more, IL-13 was selected for positive control for M2 macrophages polarization (Zhang et al., 2018). The results demonstrated that the mRNA level of Arg1, Ym1 and Mcr1 gene was significantly upregulated after RAW264.7 cells treated with VYAC (25, 50 and 100 μg/ml) for 24 h ($p < 0.05$) (Fig. 4A, B and C). Next, we used western blot to analyze the expression of Arg1 and Ym1 in RAW264.7 cells treated with VYAC (25, 50 and 100 μg/ml) for 24 h. The results showed that VYAC enhanced Arg1 and Ym1 expression to different extent (Fig. 4D and E). Further, we used flow cytometry to detect CD206 and CD86 expression, which represented M1 and M2 macrophage specific marks respectively. The results displayed that VYAC (25, 50 and 100 μg/ml) could significantly promote macrophage polarization to M2 phenotype by increased CD206 expression (Fig. 4F). Whereas, VYAC (25, 50 and 100 μg/ml) display little effects on M1 macrophage polarization as slightly changes of CD86 expression (Fig. 4G). these data indicate that VYAC is able to promote M2 macrophage polarization, but slightly on M1 macrophage polarization.

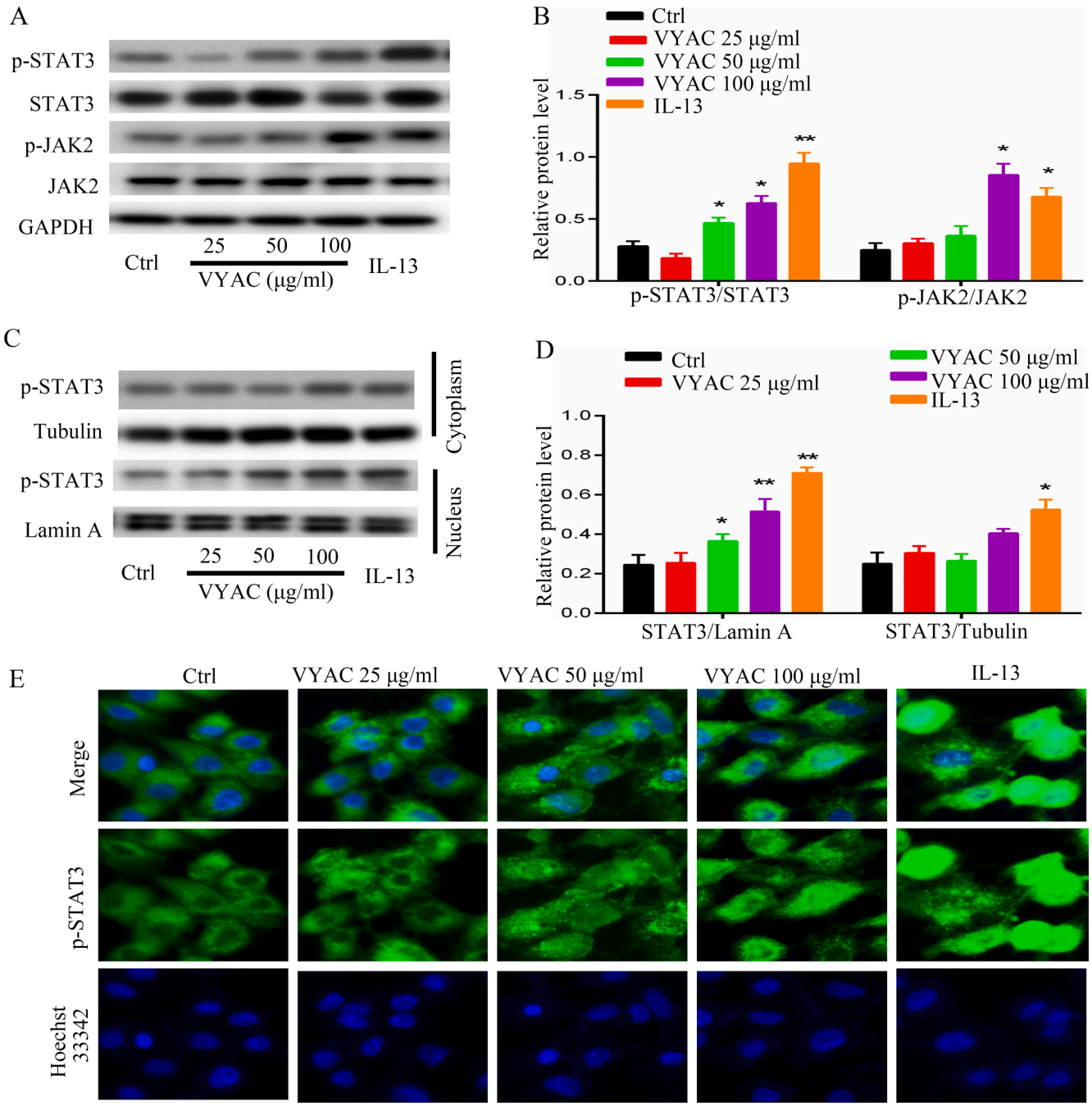

Fig. 5. VYAC activated JAK2/STAT3 signaling pathway in RAW264.7 cells. RAW264.7 cells were treated with VYAC (25, 50 100 μg/ml) or IL-13 (10 ng/ml). Western blot was used for the analysis the phosphorylation level of JAK2 and STAT3 protein (A and B). protein was separated from nucleus and cytoplasm, then phosphorylation level of STAT3 protein was detected (C and D). Immunofluorescence was used to analyze the nucleus translocation of STAT3 (E). Data are shown as mean ± SD ($n = 3$). *$p < 0.05$ and **$p < 0.01$ *vs.* control group (Ctrl).

VYAC activates JAK2/STAT3 signaling pathway in RAW264.7 cells

Recent studies have revealed that JAK2/STAT3 signaling pathway is very crucial in M2 macrophage re-programming (de Jonge et al., 2005; Wang et al., 2021). So, we explored this signaling pathway in VYAC modulated M2 macrophage activation. First, we measured the protein phosphorylation levels of both JAK2 and STAT3 through western blot. The results displayed that VYAC could significantly increase protein phosphorylation of JAK2 and STAT3 in a dose-dependent manner (Fig. 5A and B). STAT3 would translocate to nucleus after protein phosphorylation. So, we separate proteins from nucleus and cytoplasm and detected protein phosphorylation levels of STAT3. The results showed that VYAC increased STAT3 phosphorylation levels in nucleus in a dose-dependent manner, but had little influence on STAT3 phosphorylation levels in cytoplasm (Fig. 5C and D). Furthermore, immunofluorescence assay also demonstrated that VYAC promoted STAT3 nuclear translocation with strong fluorescence in a dose-dependent manner (Fig. 5E). These data illustrated that VYAC activated the JAK2/STAT3 molecular pathway to enhance STAT3 translocate to nucleus.

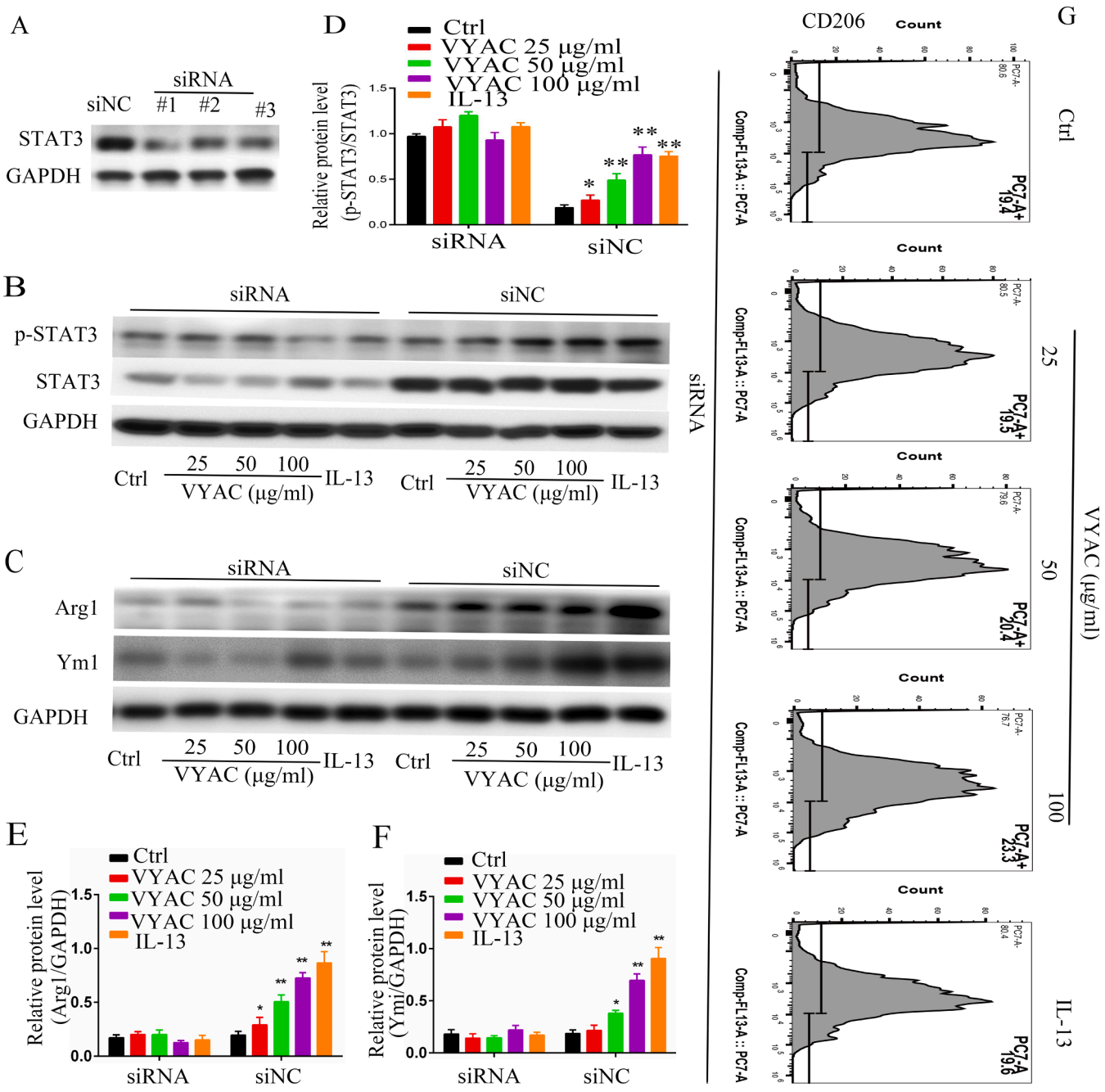

Fig. 6. VYAC promoted M2 macrophages polarization through JAK2/STAT3 signaling pathway. RAW264.7 cells were treated with STAT3 siRNA and the protein expression was analyzed by western blot (A). RAW264.7 cells were transfected STAT3 siRNA (or not), then treated with VYAC (25, 50 100 μg/ml) or IL-13 (10 ng/ml), the phosphorylation level of STAT3 protein was analyzed by western blot (B and D). The protein expression of M2 macrophages related protein Ym1 and Arg1 was analyzed by western blot (C, E and F). The population of M2 macrophages ($CD206^{+}$) was analyzed by flow cytometry (G). Data are shown as mean ± SD ($n = 3$). $^{*}p < 0.05$ and $^{**}p < 0.01$ *vs.* control group (Ctrl).

JAK2/STAT3 signaling pathway plays a crucial role in M2 macrophage activation by VYAC in both RAW264.7 cells and BMDM cells

To further explore the relationship between JAK2/STAT3 signaling pathway and M2 macrophage polarization, we used STAT3 specific interfering RNA (siRNA) to knocking down STAT3 in RAW264.7 cells, followed by treatment with different concentrations of VYAC (25, 50 and 100 μg/ml). The results displayed that STAT3 was successfully knocking down after STAT3 specific interfering RNA (Fig. 6A). As a result, VYAC induced STAT3 protein phosphorylation was significantly inhibited following STAT3 knocking down, while the ability of VYAC for enhancing STAT3 translocate to nucleus was suppressed (Fig. 6B and D). Furthermore, M2 macrophages related protein of Arg1 and Ym1 were also restrained after STAT3 knocking down (Fig. 6C, E and F). Meanwhile, flow cytometry was used to detect CD206, a M2 macrophage specific mark. The results showed that CD206, suggesting that the ability of VYAC in promoting M2 macrophage polarization was blocked following STAT3 knocking down (Fig. 6G). These data clearly demonstrate that JAK2/STAT3 signaling pathway plays a crucial role in M2 macrophage activation by VYAC.

To further verify the importance of JAK2/STAT3 signaling pathway on M2 macrophage polarization and the anti-inflammatory effects and by VYAC. We isolated bone-marrow-derived macrophages (BMDMs) for further validation. The isolated primary BMDMs were added M-CSF and

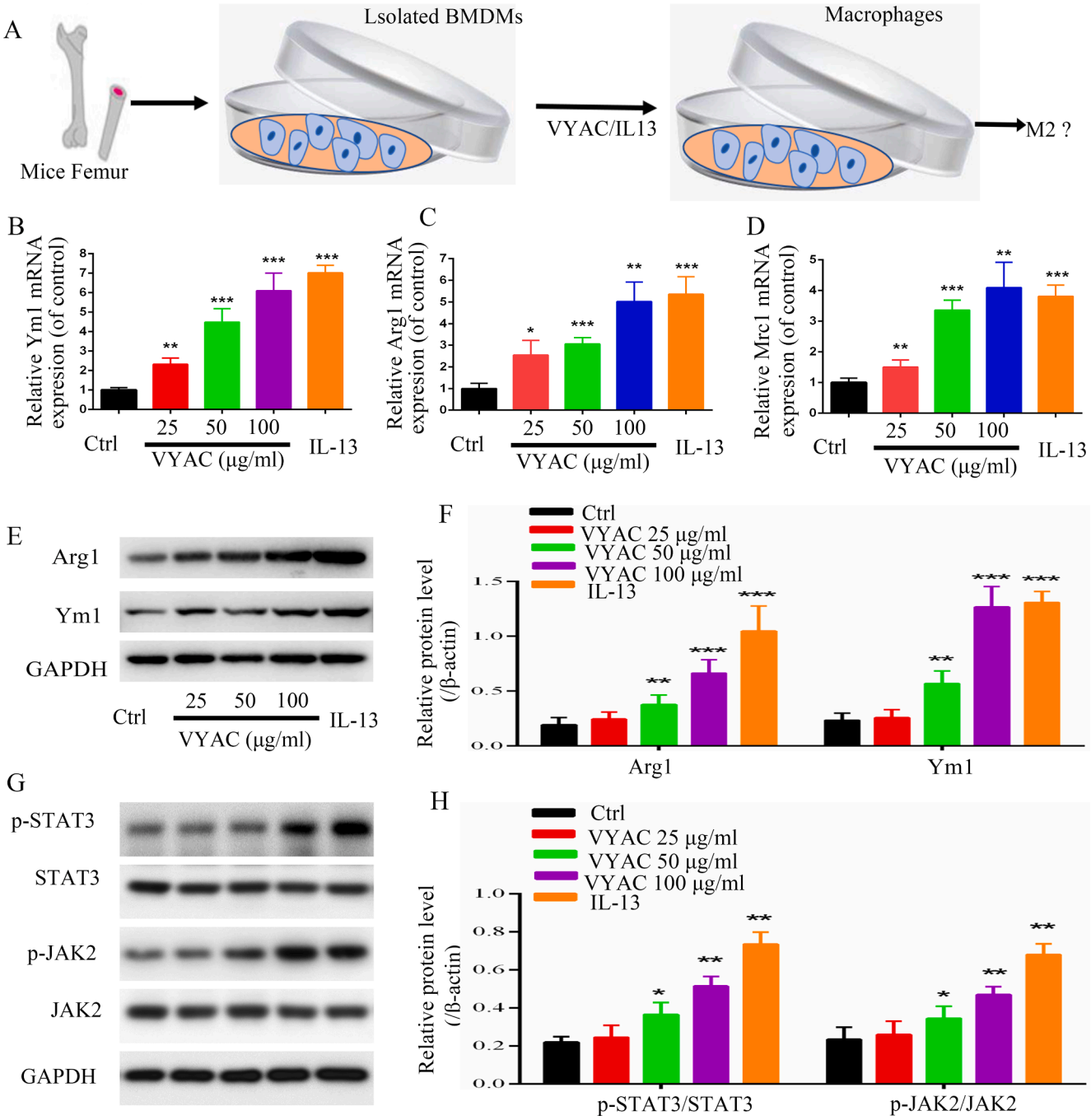

Fig. 7. VYAC promoted M2 macrophages polarization and activated JAK2/STAT3 signaling pathway in BMDM cells. Bone-marrow-derived macrophages (BMDMs) were isolated from mice femur and treated with VYAC (25, 50 100 μg/ml) or IL-13 (10 ng/ml). (A) Schematic diagram of BMDMs isolation and M2 macrophages polarization identification. The mRNA level of M2 macrophages related genes Ym1 (B), Arg1 (C), Mrc1(D) was analyzed by qRT-PCR. The protein expression of M2 macrophages related protein Ym1 and Arg1 was analyzed by western blot (E and F). The phosphorylation level of JAK2 and STAT3 protein were also analyzed by western blot. Data are shown as mean ± SD ($n = 3$). $^{*}p < 0.05$, $^{**}p < 0.01$ and $^{***}p < 0.001$ *vs.* control group (Ctrl).

cultured 7 days to get mature BMDMs. First, the cytotoxicity of VYAC on BMDMs was investigated. The results showed that there is no cytotoxicity on BMDMs cells below the dose of 400 μg/ml, and a little cytotoxicity at the dose of 800 μg/ml (**Fig. S2 B**). Then, the cells were stimulated with different concentrations of VYAC (25, 50 and 100 μg/ml) of IL-13 (10 ng/ml) for 24 h, qRT-PCR and western blot were used to analyze macrophage polarization (Fig. 7A). The results demonstrated that the mRNA level of M2 macrophage related genes (Arg1, Ym1 and Mcr1) was significantly upregulated in a dose-dependent manner after stimulated with VYAC (25, 50 and 100 μg/ml) ($p < 0.05$) (Fig. 7B, C and D). The expression of Arg1 and Ym1 protein was also increased in a dose-dependent manner after stimulated with VYAC (25, 50 and 100 μg/ml) ($p < 0.05$) (Fig. 7E and F). The protein phosphorylation levels of JAK2 and STAT3 were also increased in a dose-dependent manner after stimulated with VYAC (25, 50 and 100 μg/ml) ($p < 0.05$) (Fig. 7G and H). These data suggested that VYAC also promote M2 macrophage polarization and activated JAK2/STAT3 signaling pathway in BMDMs.

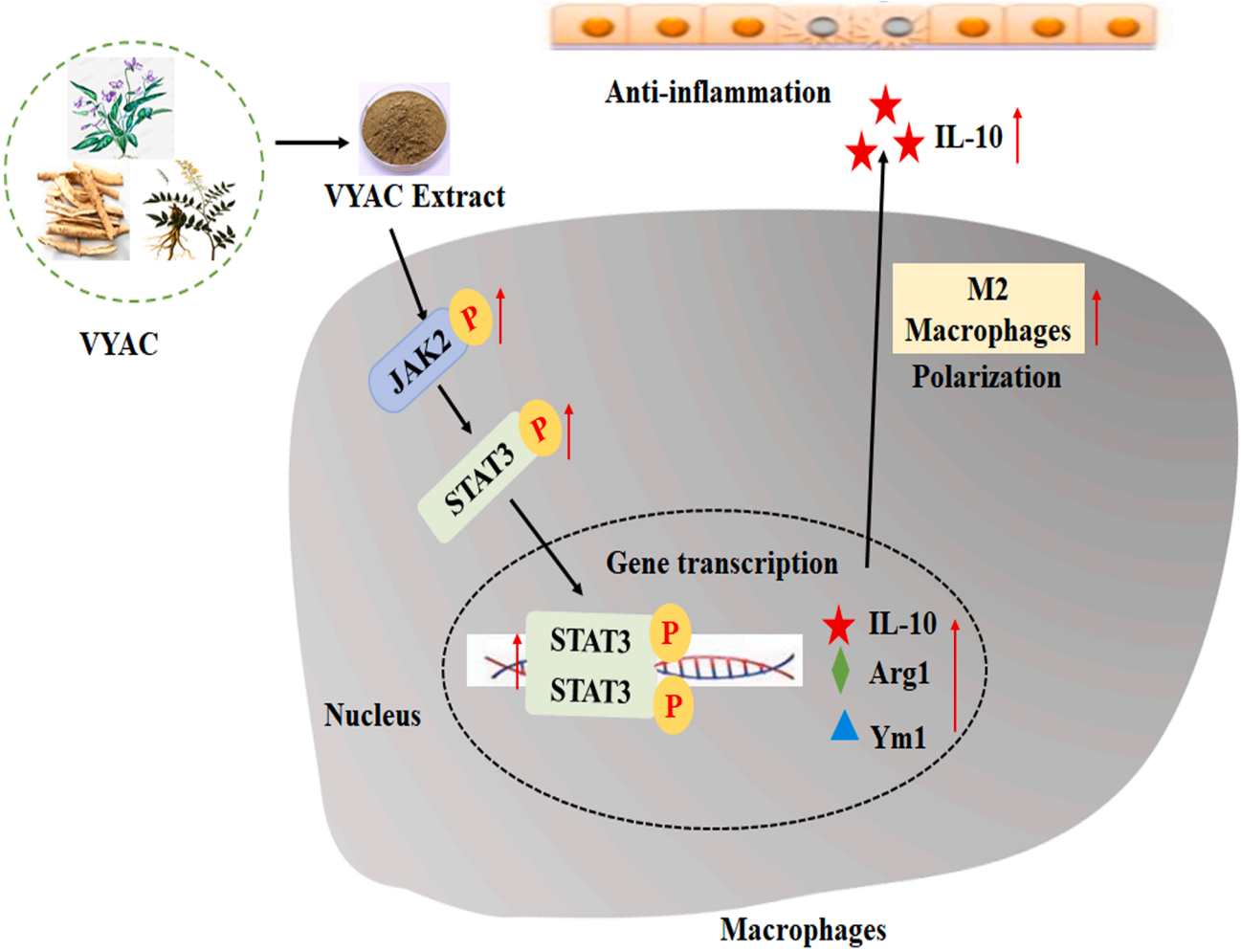

Fig. 8. The possible mechanism of VYAC promotes M2 macrophages polarization.

Discussion

AD characterized by intense itch and recurrent skin lesions, alone with abnormal immune system, is a typical inflammatory skin disease (Schultze et al., 2015). Despite the effects of current drugs for AD have been achieved, however, the prevalence of AD is still increasing (Abuabara et al., 2018). The pathophysiology of AD has been well advanced over the past decades, but much still remains inexplicit. It involves a dysfunction epidermal barrier, skin microbiome and immune dysfunction (Langan et al., 2020). The key pathogenesis of AD is cutaneous inflammation; the lesion skin of AD patient shows a T-cell infiltration, dendritic cells, innate lymphoid cells and Th2 cells activated. The release of IL-10, IL-4 and IL-13 promoted macrophages polarization and activated transcription (STAT3) pathway (Weidinger et al., 2018). Macrophages play a key role in various diseases associated with chronic inflammation, including skin disorder (Schultze et al., 2015). Macrophage activation includes two pathways, classical M1 pathway induced by interferon-γ (IFN-γ) and lipopolysaccharide (LPS) that produces large amounts of pro-inflammatory factors, which exacerbates disease progression. While, M2 macrophages, induced IL-4 or IL-13 expressed IL-10, is thought to an anti-inflammatory phenotype. Our results found that DNCB-induced AD mice displayed skin lesion, increased level of proinflammatory factors and enhanced macrophages infiltration. What's more, VYAC ameliorated DNCB-induced AD mice skin lesion, decreased the level of proinflammatory factors, inhibited macrophages infiltration and promoted M2 macrophages polarization.

AD treatment first involves improving symptoms, then establishing long-term diseases control including skin barrier restoration, avoidance of trigger factors and reducing inflammation (Eichenfield et al., 2017). Moisturizers increased hydration, reduced xerosis, itch and flares, which could improve barrier function, and is good for AD treatment (van Zuuren et al., 2017). However, for severity AD, only moisturizers are not enough, it must be combined with anti-inflammatory agents, such as glucocorticoids and immunosuppressants (Jung et al., 2015). However, the serious side effects and the risk of resistance or rebound makes AD treatment not very satisfactory (Wang et al., 2020). So, it's urgent to seek a safe and effective alternative and complementary medication. Chinese herbal medicine is a good choice for its safety. In our current study, *Viola yedoensis* Makino formula (VYAC) consisting of three herbs including *Viola yedoensis* Makino, *Sophora flavescens* Aiton and *Dictamnus dasycarpus* Turcz, is a clinical prescription for skin disease. We found that VYAC has a good effect on AD treatment.

JAK/STAT, a classical signaling pathway which is related to cell survival, immunosuppression, plays an important role in inflammatory biological response (Kabiri et al., 2020). Lots of cytokine signal through JAK2/STAT3, JAK2 as a foremost JAK transmitting intracellular signals of cytokines including IL-10, IL-6 and IFN-γ (Che et al., 2019). Moreover, JAK2/STAT3 activation resulted in T regulatory cell population and M1 to M2 macrophage polarization (Li et al., 2014). Researches demonstrated that activated JAK2/STAT3 signaling pathway in macrophages is involved in immune response (Tao et al., 2015). Therefore, seeking drugs capable of modulating this pathway is crucial. Zhang and their group found that (+)-Borneol improves the efficacy of edaravone against DSS-induced colitis through enhancing M2 macrophages activation via

JAK2-STAT3 pathway (Zhang et al., 2017). Wang and their group discovered that Lenalidomide regulates central nervous system autoimmunity by promoting M2 macrophages polarization (Weng et al., 2018). Lu and their group demonstrated that Huanglian Jiedu Decoction ameliorates DSS-induced colitis in mice via the JAK2/STAT3 signaling pathway (Lu et al., 2020). In our study, we found that VYAC was capable of activating JAK2/STAT3 signaling pathway that promotes M2 macrophages polarization, and in this manner ameliorated DNCB-induced AD.

Macrophages are phenotypically dynamic ranging from a resting ramified steady-state (Mo) to a pro-inflammatory phenotype (M1) or anti-inflammatory phenotype (M2), and display different morphology and functions (Zhou et al., 2020). Many studies have showed that various factors and signaling or drugs can stimulate macrophage differentiation. Li et al., found that elevated CDKN2B-AS1 in macrophages promotes the M1 polarization and inhibited the M2 polarization of macrophages by the CDKN2B-AS1/ MIR497/TXNIP axis (Li et al., 2021). Zheng et al., discovered that ETS-like transcription factor 4 (ELK4) induced macrophage M2 polarization via the KDM5A-PJA2-KSR1 axis, promoting the progression of gastric cancer. (Zheng et al., 2021). Deng et al., found that M2 macrophages were polarized by ovarian cancer stem cells through the PPARγ/NF-κB pathway (Deng et al., 2015). RAW264.7 as an innate macrophage (M0), can be polarized to M1 or M2 macrophages. In our current study, we found that VYAC ameliorated DNCB-induced AD by inducing M2 macrophages polarization through the JAK2/STAT3 signaling pathway (Fig. 8).

Conclusion

Taken together, this study discovered that a Chinese medicine VYAC could significantly ameliorate skin lesion of DNCB-induce AD mice, while the anti-inflammatory mechanisms of this folk medicine were explored in various cell lines. The results demonstrated that VYAC could improve the typical symptoms of AD, ameliorate skin lesion of AD mice, activate JAK2/STAT3 signaling pathway, promote M2 macrophages polarization, and restrain inflammatory factors release. All these findings provide powerful evidence for supporting the efficacy of VYAC in the treatment of AD.

Funding

This research was funded by the National Natural Science Foundation of China (81,922,070, 81,973,286, 81,703,880), Shanghai Science and Technology Innovation Action Plans (20S21901500 & 20S21900900) supported by Shanghai Science and Technology Committee, Innovation Team and Talents Cultivation Program of National Administration of Traditional Chinese Medicine (ZYYCXTD-D-202,004), Science and Technology Innovation Project of Putuo District Health System (ptkwws202204) and Research Foundation for the Shanghai Hospital Pharmacy (2019-YY-09).

Author statement

Guangbo Ge:study conception, design, and editing.

Hongping Deng: study conception, design, review and editing;

Yi Yuan: study conception, design, review and editing;

Hairong Zeng and Bei Zhao: designed and performed the overall experiments and prepared the manuscript.

Die Zhang and Xing Rui: acquisition, analysis of data and performed data processing.

Xudong Hou, Xingxing Chen and Benrui Zhang: analyzed the data and revised the manuscript

Declaration of Competing Interest

The authors declare no conflict of interest.

Supplementary materials

Supplementary material associated with this article can be found, in the online version, at doi:10.1016/j.phymed.2022.154228.

References

Abuabara, K., Yu, A.M., Okhovat, J.P., Allen, I.E., Langan, S.M., 2018. The prevalence of atopic dermatitis beyond childhood: a systematic review and meta-analysis of longitudinal studies. Allergy 73 (3), 696–704.
Ahmed, A., Solman, L., Williams, H.C., 2018. Magnitude of benefit for topical crisaborole in the treatment of atopic dermatitis in children and adults does not look promising: a critical appraisal. Br. J. Dermatol. 178 (3), 659–662.
Bieber, T., 2021. Atopic dermatitis: an expanding therapeutic pipeline for a complex disease. Nat. Rev. Drug Discov. 21 (1), 21–40.
Bos, J.D., Van Leent, E.J., Sillevis Smitt, J.H., 1998. The millennium criteria for the diagnosis of atopic dermatitis. Exp. Dermatol. 7 (4), 132–138.
Campana, R., Dzoro, S., Mittermann, I., Fedenko, E., Elisyutina, O., Khaitov, M., Karaulov, A., Valenta, R., 2017. Curr. Opin. Allergy Clin. Immunol. 17 (4), 269–277.
Che, Q., Xiao, X., Liu, M., Lu, Y., Dong, X., Liu, S., 2019. IL-6 promotes endometrial cancer cells invasion and migration through signal transducers and activators of transcription 3 signaling pathway. Pathol. Res. Pract. 215 (6), 152392.
de Jonge, W.J., van der Zanden, E.P., The, F.O., Bijlsma, M.F., van Westerloo, D.J., Bennink, R.J., Berthoud, H., Uematsu, S., Akira, S., van den Wijngaard, R.M., Boeckxstaens, G.E., 2005. Stimulation of the vagus nerve attenuates macrophage activation by activating the Jak2-STAT3 signaling pathway. Nat. Immunol. 6 (8), 844–851.
Deng, X., Zhang, P., Liang, T., Deng, S., Chen, X., Zhu, L., 2015. Ovarian cancer stem cells induce the M2 polarization of macrophages through the PPARγ and NF-κB pathways. Int. J. Mol. Med. 36 (2), 449–454.
Eichenfield, L.F., Ahluwalia, J., Waldman, A., Borok, J., Udkoff, J., Boguniewicz, M., 2017. Current guidelines for the evaluation and management of atopic dermatitis: a comparison of the joint task force practice parameter and american academy of dermatology guidelines. J. Allergy Clin. Immunol. 139 (4S), S49–S57.
Girolomoni, G., de Bruin-Weller, M., Aoki, V., Kabashima, K., Deleuran, M., Puig, L., Bansal, A., Rossi, A.B., 2021. Nomenclature and clinical phenotypes of atopic dermatitis. Ther. Adv. Chronic Dis. 12, 20406223211002979.
Gür Çetinkaya, P., Şahiner, Ü.M., 2019. Childhood atopic dermatitis: current developments, treatment approaches, and future expectations. Turk. J. Med. Sci. 49 (4), 963–984.
Hristodorov, D., Mladenov, R., von Felbert, V., Huhn, M., Fischer, R., Barth, S., Thepen, T., 2015. Targeting CD64 mediates elimination of M1 but not M2 macrophages *in vitro* and in cutaneous inflammation in mice and patient biopsies. MAbs 7 (5), 853–862.
Halling-Overgaard, A.S., Kezic, S., Jakasa, I., Engebretsen, K.A., Maibach, H., Thyssen, J. P., 2017. 2017. Skin absorption through atopic dermatitis skin: a systematic review. Br. J. Dermatol. 177 (1), 84–106.
Hon, K.L., Kung, J.S.C., Ng, W.G.G., Leung, T.F., 2018. Emollient treatment of atopic dermatitis: latest evidence and clinical considerations. Drugs Context 7, 212530.
Irvine, A.D., McLean, W.H., Leung, D.Y., 2011. Filaggrin mutations associated with skin and allergic diseases. N Engl. J. Med. 365 (14), 1315–1327.
Jung, K.E., Lee, Y.J., Ryu, Y.H., Kim, J.E., Kim, H.S., Kim, B.J., Kang, H., Park, Y.M., 2015. Effects of topically applied rapamycin and mycophenolic acid on TNCBinduced atopic dermatitis-like skin lesions in NC/Nga mice. Int. Immunopharm. 26 (2), 432–438.
Kong, L., Lin, X., Huang, C., Ma, T., Meng, X., Hu, C., Wang, Q., Liu, Y., Shi, Q., Li, J., 2019. Hesperetin derivative-12 (HDND-12) regulates macrophage polarization by modulating JAK2/STAT3 signaling pathway. Chin. J. Nat. Med. 17 (2), 122–130.
Kabiri, M., Hemmatpour, A., Zare, F., Hadinedoushan, H., Karimollah, A., 2020. Paroxetine modulates immune responses by activating a JAK2/STAT3 signaling pathway. J. Biochem. Mol. Toxicol. 34 (5), e22464.
Karuppagounder, V., Arumugam, S., Thandavarayan, R.A., Sreedhar, R., Giridharan, V. V., Pitchaimani, V., Afrin, R., Harima, M., Krishnamurthy, P., Suzuki, K., Nakamura, M., Ueno, K., Watanabe, K., 2016. Naringenin ameliorates skin inflammation and accelerates phenotypic reprogramming from M1 to M2 macrophage polarization in atopic dermatitis NC/Nga mouse model. Exp. Dermatol. 25 (5), 404–407.
Langan, S.M., Irvine, A.D., Weidinger, S., 2020. Atopic dermatitis. Lancet 396 (10247), 345–360.
Li, L., Xu, T., Huang, C., Peng, Y., Li, J., 2014. NLRC5 mediates cytokine secretion in RAW264.7 macrophages and modulated by the JAK2/STAT3 pathway. Inflammation 37 (3), 835–847.
Lu, Z., Xiong, W., Xiao, S., Lin, Y., Yu, K., Yue, G., Liu, Q., Li, F., Liang, J., 2020. Huanglian Jiedu Decoction ameliorates DSS-induced colitis in mice via the JAK2/STAT3 signalling pathway. Chin. Med. 15, 45.
Li, Y., Gu, C., Liu, G., Yu, Y., Xu, J., 2021. Polarization of rheumatoid macrophages is regulated by the CDKN2B-AS1/MIR497/TXNIP axis. Immunol. Lett. 239, 23–31.
Lee, S.B., Park, H., Lee, J.E., Kim, K.S., Jeon, Y.H., 2020. *In vivo* optical reporter-gene-based imaging of macrophage infiltration of DNCB-induced atopic dermatitis. Int. J. Mol. Sci 21 (17), 6205.
McAleer, M.A., Irvine, A.D., 2013. The multifunctional role of filaggrin in allergic skin disease. J. Allergy Clin. Immunol. 131 (2), 280–291.
Nakai, K., 2021. Multiple roles of macrophage in skin. J Dermatol Sci 104 (1), 2–10.

Nakagawa, H., Nemoto, O., Igarashi, A., Saeki, H., Kaino, H., Nagata, T., 2020. Delgocitinib ointment, a topical Janus kinase inhibitor, in adult patients with moderate to severe atopic dermatitis: a phase 3, randomized, double-blind, vehicle-controlled study and an open-label, long-term extension study. J. Am. Acad. Dermatol. 82 (4), 823–831.

Qader, M., Xu, J., Yang, Y., Wu, X., Liu, Y., Cao, S., 2021. Chemistry behind the immunomodulatory activity of astragalus membranaceus. Chin. Med. Cult. 4 (4), 201–210. https://doi.org/10.4103/CMAC.CMAC_40_21.

Saeki, H., Furue, M., Furukawa, F., Hide, M., Ohtsuki, M., Katayama, I., Sasaki, R., Suto, H., Takehara, K., 2009. Guidelines for management of atopic dermatitis. J. Dermatol. 36 (10), 563–577.

Schultze, J.L., Schmieder, A., Goerdt, S., 2015. Macrophage activation in human diseases. Semin. Immunol. 27 (4), 249–256.

Trouplin, V., Boucherit, N., Gorvel, L., Conti, F., Mottola, G., Ghigo, E., 2013. Bone marrow-derived macrophage production. J. Vis. Exp. (81), e50966.

Tao, Z., Cheng, M., Wang, S., Lv, W., Hu, H., Li, C., Cao, B., 2015. JAK2/STAT3 pathway mediating inflammatory responses in heatstroke-induced rats. Int. J. Clin. Exp. Pathol. 8 (6), 6732–6739.

Thomsen, S.F., Ulrik, C.S., Kyvik, K.O., Hjelmborg, J.B., Skadhauge, L.R., Steffensen, I., Backer, V., 2007. Importance of genetic factors in the etiology of atopic dermatitis: a twin study. Allergy Asthma Proc. 28 (5), 535–539.

Tsakok, T., Woolf, R., Smith, C.H., Weidinger, S., Flohr, C., 2019. Atopic dermatitis: the skin barrier and beyond. Br. J. Dermatol. 180 (3), 464–474.

van Zuuren, E.J., Fedorowicz, Z., Arents, B.W.M., 2017. Emollients and moisturizers for eczema: abridged Cochrane systematic review including GRADE assessments. Br. J. Dermatol. 177 (5), 1256–1271.

Wallach, D., Taïeb, A., 2014. Atopic dermatitis/atopic eczema. Chem. Immunol. Allergy 100, 81–96.

Weidinger, S., Beck, L.A., Bieber, T., Irvine, A.D., 2018. Atopic dermatitis. Nat. Rev. Dis. Primers 4 (1), 2.

Wang, X., Li, S., Liu, J., Kong, D., Han, X., Lei, P., Xu, M., Guan, H., Hou, D., 2020. Ameliorative effects of sea buckthorn oil on DNCB induced atopic dermatitis model mice via regulation the balance of Th1/Th2. BMC Complementary Med. Therapies 20 (1), 263.

Weng, Q., Wang, J., Wang, J., Wang, J., Sttar, F., Zhang, Z., Zheng, J., Xu, Z., Zhao, M., Liu, X., Yang, L., Hao, G., Fang, L., Lu, Q.R., Yang, B., He, Q., 2018. Lenalidomide regulates CNS autoimmunity by promoting M2 macrophages polarization. Cell Death Dis. 9 (2), 251.

Wang, G., Liu, X., Li, X., Zhao, Y., 2021. Suppression of PAPP-A mitigates atherosclerosis by mediating macrophage polarization via STAT3 signaling. Biochem. Biophys. Res. Commun. 543, 29–37.

Weidinger, S., Baurecht, H., Schmitt, J., 2017. A 5-year randomized trial on the safety and efficacy of pimecrolimus in atopic dermatitis: a critical appraisal. Br. J. Dermatol. 177 (4), 999–1003, 2017.

Yu, Q., Zeng, K., Ma, X., Song, F., Jiang, Y., Tu, P., Wang, X., 2016. Resokaempferol-mediated anti-inflammatory effects on activated macrophages via the inhibition of JAK2/STAT3, NF-κB and JNK/p38 MAPK signaling pathways. Int. Immunopharmacol. 38, 104–114.

Yuan, F., Fu, X., Shi, H., Chen, G., Dong, P., Zhang, W., 2014. Induction of murine macrophage M2 polarization by cigarette smoke extract via the JAK2/STAT3 pathway. PLoS ONE 9 (9), e107063.

Zeng, H., Zhao, B., Rui, X., Jia, G., Wu, Y., Zhang, D., Yu, H., Zhang, B., Yuan, Y., 2021. A TCM formula VYAC ameliorates DNCB-induced atopic dermatitis via blocking mast cell degranulation and suppressing NF-κB pathway. J Ethnopharmacol 280, 114454.

Zeng, L., Liu, Y., Xing, C., Xing, C., Huang, Y., Sun, X., Sun, G., 2020. Saponin from Periploca forrestii Schltr Mitigates Oxazolone-Induced Atopic Dermatitis via Modulating Macrophage Activation. Mediators Inflamm 2020, 4346367.

Zhang, X., Xu, F., Liu, L., Feng, L., Wu, X., Shen, Y., Sun, Y., Wu, X., Xu, Q., 2017. (+)-Borneol improves the efficacy of edaravone against DSS-induced colitis by promoting M2 macrophages polarization via JAK2-STAT3 signaling pathway. Int. Immunopharmacol. 53, 1–10.

Zeng, H., Wang, B., Zhao, Z., Zhang, Q., Liang, M., Yao, Y., Bian, K., Zhang, W., 2016. Effects of Viola yedoensis Makino anti-itching compound on degranulation and cytokine generation in RBL-2H3 mast cells. J. Ethnopharmacol. 189, 132–138.

Zhang, X., Liu, M., Qiao, L., Zhang, X., Liu, X., Dong, M., Dai, H., Ni, M., Luan, X., Guan, J., Lu, H., 2018. Ginsenoside Rb1 enhances atherosclerotic plaque stability by skewing macrophages to the M2 phenotype. J. Cell Mol. Med. 22 (1), 409–416.

Zhang, F., Huang, J., Liu, W., Wan, g C.R., Liu, Y.F., Tu, D.Z., Liang, X.M., Yang, L., hang, W.D., Chen, H.Z., Ge, G.B., 2021. Inhibition of drug-metabolizing enzymes by Qingfei Paidu decoction: implication of herb-drug interactions in COVID-19 pharmacotherapy. Food Chem. Toxicol. 19 (149), 111998.

Zhou, J., Li, Z., Wu, T., Zhao, Q., Zhao, Q., Cao, Y., 2020. LncGBP9/miR-34a axis drives macrophages toward a phenotype conducive for spinal cord injury repair via STAT1/STAT6 and SOCS3. J. Neuroinflammation 17 (1), 134.

Zheng, L., Xu, H., Di, Y., Chen, L., Liu, J., Kang, L., Gao, L., 2021. ELK4 promotes the development of gastric cancer by inducing M2 polarization of macrophages through regulation of the KDM5A-PJA2-KSR1 axis. J. Transl. Med. 19 (1), 342.